COMMISSIONING OF A HIGH-BRIGHTNESS PHOTOINJECTOR FOR COMPTON SCATTERING X-RAY SOURCES*

S. G. Anderson†, C. P. J. Barty, D. J. Gibson, F. V. Hartemann, M. Messerly, M. Shverdin,
C. W. Siders, A. M. Tremaine, LLNL, Livermore, CA 94550, USA
H. Badakov, P. Frigola, A. Fukasawa, B. OShea, J. B. Rosenzweig
UCLA, Los Angeles, CA 90095, USA

Abstract

Compton scattering of intense laser pulses with ultra-relativistic electron beams has proven to be an attractive source of high-brightness x-rays with keV to MeV energies. This type of x-ray source requires the electron beam brightness to be comparable with that used in x-ray free-electron lasers and laser and plasma based advanced accelerators. We describe the development and commissioning of a 1.6 cell RF photoinjector for use in Compton scattering experiments at LLNL. Injector development issues such as RF cavity design, beam dynamics simulations, emittance diagnostic development, results of sputtered magnesium photo-cathode experiments, and UV laser pulse shaping are discussed. Initial operation of the photoinjector is described.

INTRODUCTION

Bright, monoenergetic beams of gamma-rays ($\Delta E/E \leq 10^{-3}$) ranging from hundreds of keV to several MeV will become important tools of future experimental investigation. In applications under development at LLNL, this type of beam will be used to induce and observe nuclear resonance fluorescence (NRF) [1]. By tuning the gamma-ray beam energy, NRF can be used to identify particular isotopes, while the energies of NRF transitions are well suited to allow the photons to penetrate materials with large areal densities. Detection systems based on NRF may be applicable to areas including nonproliferation, waste identification, and material characterization.

The x-ray source under construction at LLNL, T-REX (Thompson-Radiated Extreme X-rays), will produce 680 keV photons by colliding a 112 MeV photo-electron beam with a 355 nm, joule class laser pulse. Start-to-end simulations of this source have shown peak brightnesses of 10^{22} photons/($\mathrm{mm}^2 \times \mathrm{mrad}^2 \times \mathrm{s} \times 0.1\%\mathrm{bandwidth}$) [2]. The brightness of this source scales inversely with the square of the *geometric* emittance of the electron beam, thus making it very attractive at higher energies. This scaling also reveals the fact that optimization of the electron beam brightness is critical to the brightness of the photon source. In fact, the electron beams parameters required to achieve the photon source brightness given above are comparable with those of X-ray free-electron lasers and other advanced photo-beam applications ($\approx$ 1 mm mrad, 1 nC).

We describe here the photoinjector designed to generate the electron beam parameters required by T-REX. Radio frequency (RF) design considerations, beam dynamics simulations, low and high power tests, photo-cathode experiments, and emittance diagnostic development work are detailed. Development of a fiber-based cathode drive laser is described.

THE PHOTO-GUN

The T-REX gun, shown in Fig. 1, is a 1.6 cell photocathode gun of the BNL/SLAC/UCLA/LLNL design [3]. There are however, several key changes from previous designs [4]. First, because on-axis laser injection is planned, the 70° ports of the half cell were removed, making the half cell fully cylindrically symmetric. The full cell was also symmetrized to quadrupole moment by replacing the tuning plungers, which have been found to break down at high field and limit gun performance [5], with race-track shaped slots identical to the RF coupling slot.

Another significant change to the gun design was to increase the frequency separation of the 0- and π-modes. This modification was first implemented at SLAC in order to minimize the excitation of 0-mode fields which were

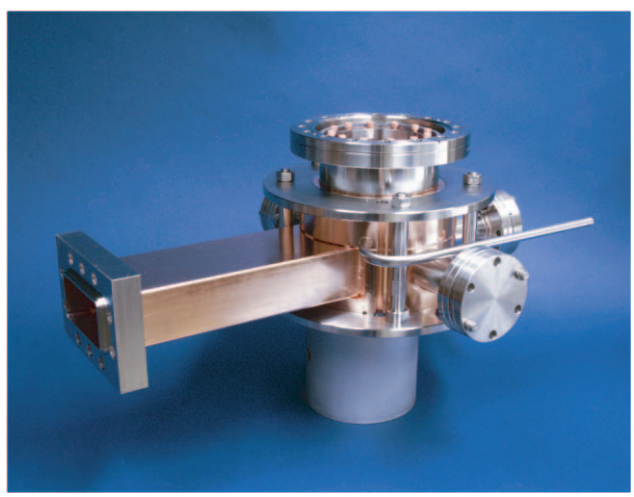

Figure 1: The T-REX photo-gun.

* This work was performed under the auspices of the U.S. Department of Energy by the University of California, Lawrence Livermore National Laboratory under contract No. W-7405-Eng-48, and by the University of California, Los Angeles under contract numbers DE-FG-98ER45693 and DE-FG03-92ER40693

† anderson131@llnl.gov

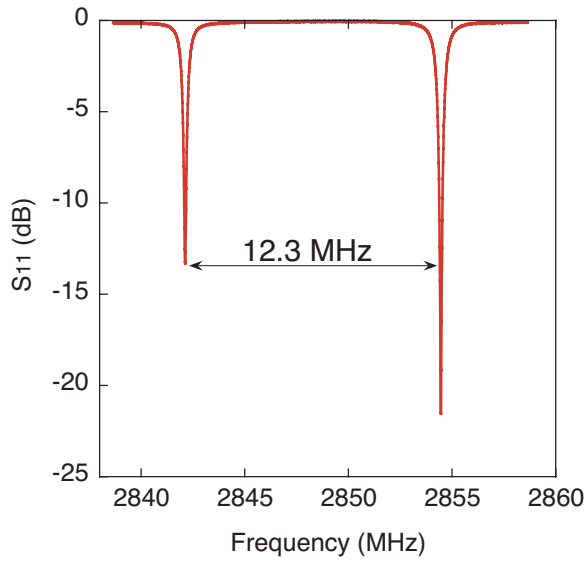

Figure 2: Network analyzer measurements of the T-REX gun showing the 0- to π-mode separation increased to 12.3 MHz.

found to have a detrimental effect on the beam emittance and energy spread [6]. The mode separation of the T-REX gun was increased to 12.3 MHz. PARMELA simulations were performed and indicate that the effect of the 0-mode is negligible at the larger mode separation, in agreement with the results of Ref. [6].

Cavity resonance and bead pull measurements were performed before and after brazing to ensure that π-mode field balance and frequency could be properly adjusted using only cathode plate deformation and temperature tuning. These measurements agreed well with 3-D HFSS simulations. The reflected power measurements of the gun installed at LLNL are shown in Fig. 2. Bead pull data indicates better than 1% field balance at the measured 12.3 MHz mode separation.

The photo-cathode, pictured in Fig. 3, consists of a copper disk which forms the half cell back plane, with a 2μm sputter-coated layer of Mg deposited in a 1cm diameter circle in the center. This cathode preparation technique builds on previous efforts [7], but with the key difference of a 150Å'adhesion-layer' of Cr used between the Cu and Mg.

The T-REX gun with sputtered Mg cathode has been RF conditioned at LLNL up to 8 MW of peak power, corresponding to approximately 107 MV/m peak accelerating field. Further conditioning is possible but will not be done until the performance of the gun and cathode can be fully evaluated. A sputtered Mg cathode was installed in an older version of the 1.6 cell gun and conditioned to 80 MV/m peak field (limited by tuner break-downs). The quantum efficiency (QE) of the cathode was measured using a frequency tripled Ti:Sapphire laser, injected 40 RF degrees from the zero crossing. The UV laser energy was then scanned and beam charge measured. The results, plotted in Fig. 4, show a QE of 1×10^{-4} at low charge. At charges

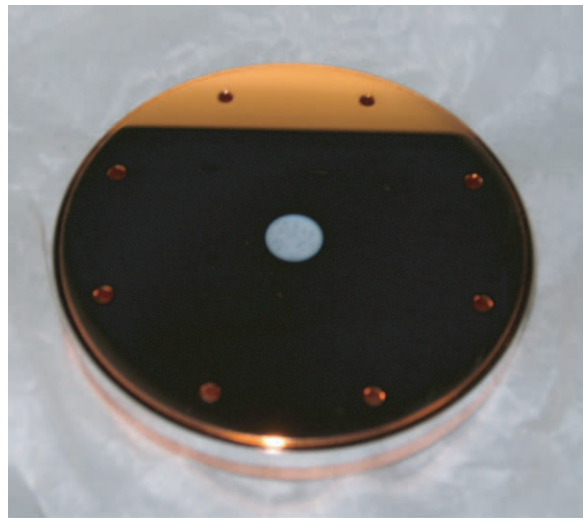

Figure 3: Image of the sputter-coated Mg photo-cathode.

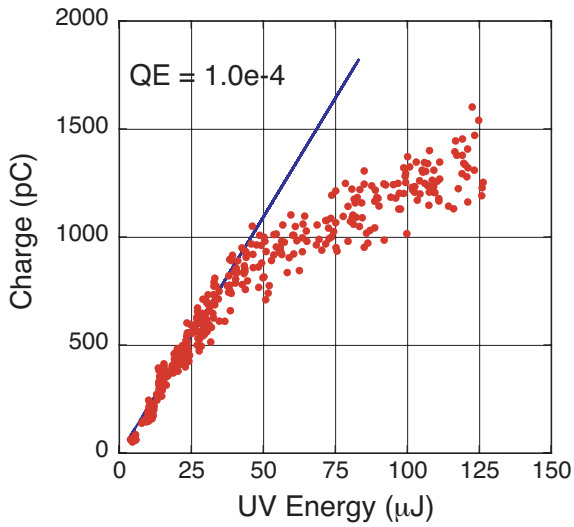

Figure 4: Charge produced using a sputtered Mg cathode plotted as a function of UV laser energy. The peak accelerating field for this measurement was 80 MV/m (limited by tuner break-down in an older gun design) and the laser was injected at 40°.

above 1 nC, the QE falls off due to the effect of longitudinal space-charge fields. This result is consistent with previous data reported for friction-welded Mg cathodes without laser cleaning [8].

The high QE of Mg enables the use of a fiber-based photo-cathode drive laser system (PDL). The T-REX PDL [9] will generate up to 500 μJ of 1047 nm, 1 ps duration light. The laser is then frequency quadrupled, sent through a pulse stacking interferometer to generate an 8 ps flat-top temporal profile, and relay imaged through an iris to the photo-cathode. In this way the 'beer-can' laser pulse shape required for emittances approaching 1 mm mrad at 1 nC of charge will be achieved.

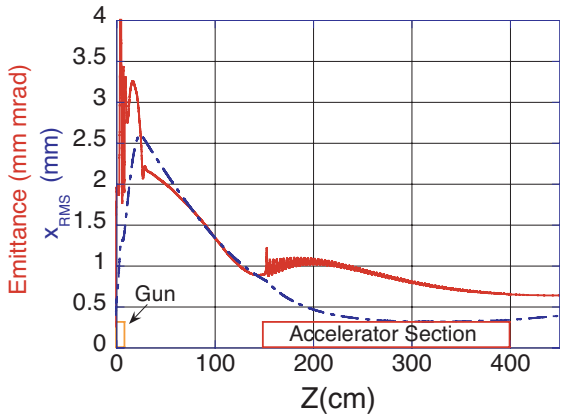

Figure 5: PARMELA simulation of the T-REX photoinjector. One nC is accelerated to 30 MeV using the gun and first accelerator section. The final normalized, rms emittance is below 1 mm mrad.

THE PHOTOINJECTOR BEAMLINE

The T-REX accelerator will generate >100 MeV electrons using 5 SLAC-type 2.5 meter traveling-wave sections. The transport line from the photo-gun to the first accelerator section has been designed both to minimize the emittance at the end of the machine and to fully diagnose the beam at low energy.

A modified version of the LCLS working point [10] is employed, which uses an 8 ps (FWHM) stacked-pulse laser profile as is anticipated using the UV interferometer. The radial profile modeled is a Gaussian cut-off at 1σ. The PARMELA simulation shown in Fig 5 tracks the beam size and normalized, rms emittance through the gun, 150cm drift region and the first accelerator section. A solenoid placed immediately downstream of the gun causes the beam to execute the typical emittance compensation oscillation [11] in both beam size and emittance, with emittance minima occurring at both the entrance and exit of the linac section.

Note that the beam is slightly converging at the entrance of the accelerator section instead of the typical design of a waist. This mismatch causes the beam size to oscillate about the invariant envelope in the section and is done to compensate for the fact that no solenoid focusing at the sections is employed. This simulation accelerates 1 nC of charge to 30 MeV, and produces a final normalized emittance of 0.7 mm mrad. No significant change in the emittance occurs with the addition of the remaining sections needed to accelerate to the T-REX design energy of 112 MeV.

The 150cm drift from photo-cathode to linac section required for proper emittance compensation is utilized to diagnose the electron beam produced by the gun. Charge is measured single-shot and non-destructively with an integrating current transformer (ICT). In addition, diagnostics exist to measure beam energy and profile, as well as

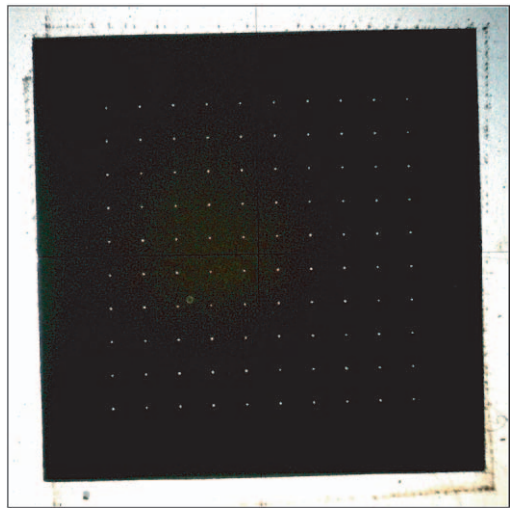

Figure 6: Comparator image of laser drilled 'pepper-pot' beam mask. An array of 20μm holes in a 0.5 mm Tungsten plate are spaced by 0.75 mm.

RF and laser parameters. Most importantly, the transverse emittance (and trace space) will be measured using a 'pepper-pot' beam mask (2-D analog to the slit mask) [12]. By observing the down-stream profile of beamlets passing through the mask the beam trace space, and therefore emittance may be reconstructed on a single-shot basis. The beam mask shown in Fig. 6 consists of an array of 20μm holes laser drilled into a 0.5mm thick tungsten plate. The geometry of the emittance diagnostic was chosen using the analysis of Ref. [12] to best measure normalized emittances in the range of 0.5 to 5 mm mrad.

REFERENCES

[1] J. Pruet *et al.*, J. Appl. Phys. **99**, 123102 (2006).

[2] F. V. Hartemann *et al.*, Phys. Rev. ST Accel. Beams **8**, 100702 (2005).

[3] D. T. Palmer, Ph. D. thesis, Stanford University (1998).

[4] A. Fukasawa *et al.*, these proceedings.

[5] A.M. Cook *et al.*, The Physics and Applications of High Brightness Electron Beams, Erice, Sicily (2005).

[6] C. Limborg *et al.*, SLAC Technical Note LCLS-TN-05-3 (2005).

[7] T. Srinivasan-Rao *et al.*, Rev. Sci. Instrum. **69**, 2292 (1998).

[8] X.J. Wang *et al.*, Proc. of LINAC 2002, pp. 142;
H. Iijima *et al.*, Proc. of LINAC 2002, pp. 166;
J.F. Schmerge *et al.*, Proc. of the 2004 FEL Conference, pp. 205.

[9] D.J. Gibson *et al.*, these proceedings.

[10] M. Ferrario *et al.*, Proc. of the 2nd ICFA Adv. Acc. Workshop on "The Physics of High Brightness Beams" (1999).

[11] L. Serafini and J.B. Rosenzweig, Phys. Rev. E **55** 7565 (1997).

[12] S.G. Anderson *et al.*, Phys. Rev. ST Accel. Beams **5**, 014201 (2002).